Chapter 5
Diagnostic Imaging in Sepsis of Pulmonary Origin

Jorge Alberto Carrillo-Bayona and Liliana Arias-Alvarez

Sepsis is defined as life-threatening organ dysfunction caused by a dysregulated host response to infection. Organ dysfunction is a clinical concept and is based on an increase of two or more points in the SOFA score [1].

Septic shock should be defined as a subset of sepsis in which particularly profound circulatory, cellular, and metabolic abnormalities are associated with a greater risk of mortality than with sepsis alone [1].

Lung infections (community- or hospital-acquired) represent the most common cause for sepsis, and in a variable percentage of patients, they are associated to acute lung injury (ALI) and acute respiratory distress syndrome (ARDS).

Diagnostic imaging plays a crucial role in the initial evaluation of patients with criteria for sepsis and suspected pulmonary infection.

The diagnosis of pneumonia is based on the presence of clinical manifestations of an infection (fever, chills, leukocytosis), signs, or symptoms located in the respiratory system (cough, increased sputum production, shortness of breath, chest pain, or abnormal lung exam) and the presence of new or changing opacities in the chest X-rays [2]. In young patients without cardiopulmonary disease, the diagnosis of pneumonia is relatively simple with the features mentioned above. However, in elderly patients or in those with underlying diseases (congestive heart failure, COPD, neoplasm, pulmonary fibrosis), the clinical picture may be variable, and pneumonia diagnosis could be complex.

The definition of severe pneumonia can be subjective and imprecise and is considered in the practice due to respiratory and/or circulatory failure requiring admission into the ICU [3].

J.A. Carrillo-Bayona (✉)
Department of Diagnostic Imaging, Universidad Nacional de Colombia,
Diagonal 57 # 1-60 ESTE, Bogotá 110911, Colombia
e-mail: jorcarbay@hotmail.com; jorcarbay@cable.net.co

L. Arias-Alvarez
Hospital Universitario San Ignacio, Bogotá, Colombia

G. Ortiz-Ruiz, C. Dueñas-Castell (eds.), *Sepsis*,
https://doi.org/10.1007/978-1-4939-7334-7_5

It is important to consider specific groups of patients with sepsis associated to pulmonary infection including immunocompromised (HIV-infected and non-HIV-infected), patients with pneumonia associated to health care, and patients with pneumonia associated to mechanical ventilation. In these contexts, the etiology of the infections varies, and radiographic manifestations can have characteristic features.

In patients with clinical signs and symptoms of respiratory infection, the chest X-ray allows confirming the diagnosis of pneumonia. On the other hand, the chest X-ray can be useful to assess response to treatment (in some patients), define a pattern suggesting specific germs (particularly TB), identify complications (empyema and ARDS) and propose a differential diagnosis.

Concepts relating to the usefulness of HRCT in patients with pneumonia have evolved. Traditionally, HRCT is used in patients with torpid clinical evolution, comorbidities, or suspected complications such as empyema, ARDS, and lung abscess. Recent studies suggest that HRCT can play a major role in patients with suspected pneumonia. Nie et al. in their work with 178 patients with community-acquired pneumonia (CAP) concluded that the effect of the treatment based on HRCT findings is not inferior to the effect of the treatment guided by microbiological characterization [4]. A series by Karhu et al. (65 patients with severe community-acquired pneumonia) discovered new HRCT findings compared to those seen on the X-rays in 60% of the patients, which generated an additional treatment conduct in 75% of the cases [5]. The retrospective nature of the trials and the scarce number of patients, currently, do not allow recommending substantial changes on the use of HRCT in patients with pneumonia. However, there is no doubt that new multidetector helical tomography techniques, with drastic reduction of ionizing radiation for the patient, can offer safe and relevant information in patients with pneumonia. Therefore, further studies are required to redefine the usefulness of HRCT for the diagnosis and follow-up of patients with suspected pneumonia.

Three classic radiographic patterns are described in patients with pneumonia including:

(a) *Focal or lobar pneumonia*. Resulting from a rapid production of fluid edema with scarce cellular reaction (Fig. 5.1).
(b) *Bronchopneumonia pattern*. Related to inflammation located in the airways and patchy alteration of adjacent lung parenchyma. With disease progression, parenchymal alterations may coalesce and form a lobar pattern (Fig. 5.2).
(c) *Interstitial pattern.* Associated to an inflammatory cellular infiltrate and edema predominantly in the lung interstitium [6] (Fig. 5.3).

It is important to bear in mind particular alterations or patterns in imaging studies that allow suggesting specific germs on certain clinical contexts.

Ground-glass pattern. Defined as increased attenuation of lung parenchyma that allows visualization of lung vessels and bronchial walls. In immunocompromised

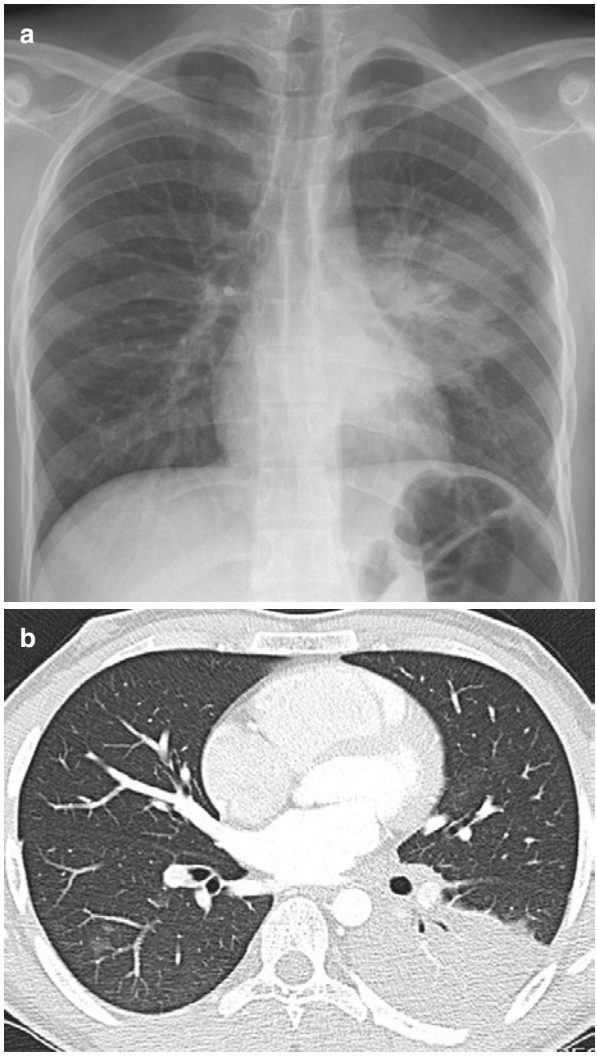

Fig. 5.1 (**a**, **b**) Focal or lobar pattern. Chest X-ray and CT of a 36-year-old man with *S. pneumoniae* infection show left lower lobe consolidation

patients, the presence of ground glass can suggest *P. jiroveci* or CMV pneumonia. Pneumonia due to *M. pneumoniae* can also be accompanied by predominant ground-glass opacities (Fig. 5.4).

Nodules. The presence of small, randomly distributed nodules (less than 10 mm in diameter) or micronodules (less than 3 mm) can suggest hematogenous dissemination of TB or mycosis (histoplasmosis). Nodules above 10 mm in diameter are not a frequent finding in patients with CAP, and their presence may suggest specific germs such as *N. asteroides*, mycosis (histoplasmosis), TB, or an alternative diagnosis (metastatic disease) (Fig. 5.5).

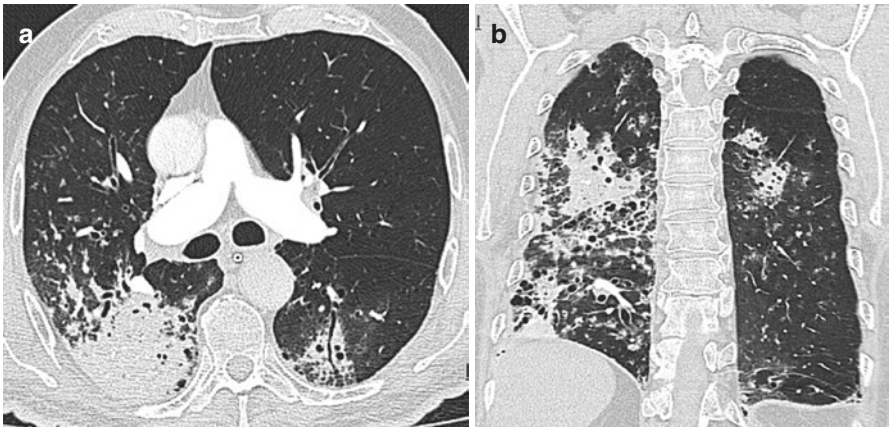

Fig. 5.2 (**a**, **b**) Bronchopneumonia pattern. Axial and coronal HRCT of a 42-year-old man with *S. aureus* infection shows bronchial wall thickening and peribronchovascular consolidation

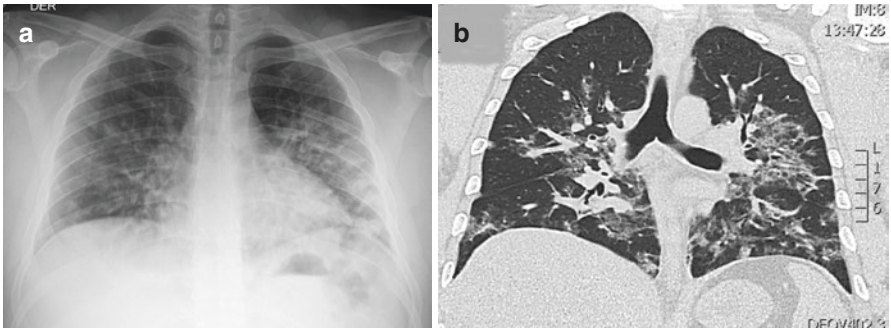

Fig. 5.3 (**a**, **b**) Interstitial pattern. Chest X-ray and coronal HRCT of a 27-year-old man with *M. pneumoniae* infection show reticular opacities (X-ray) and ground-glass opacities (HRCT)

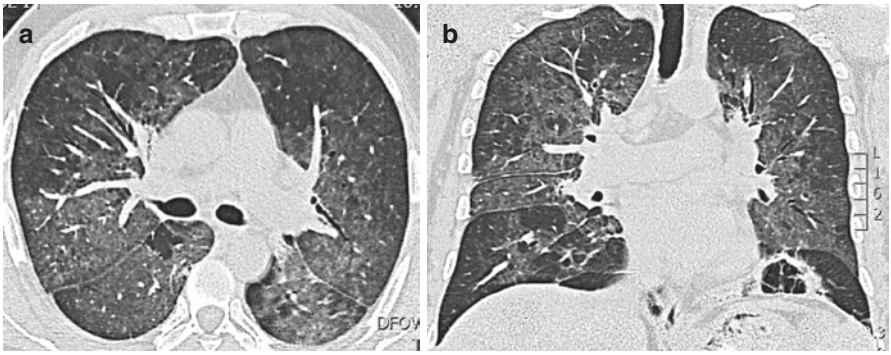

Fig. 5.4 (**a**, **b**) Ground-glass pattern. Axial and coronal HRCT of a 26-year-old man with *P. jiroveci* infection shows geographic ground-glass opacities

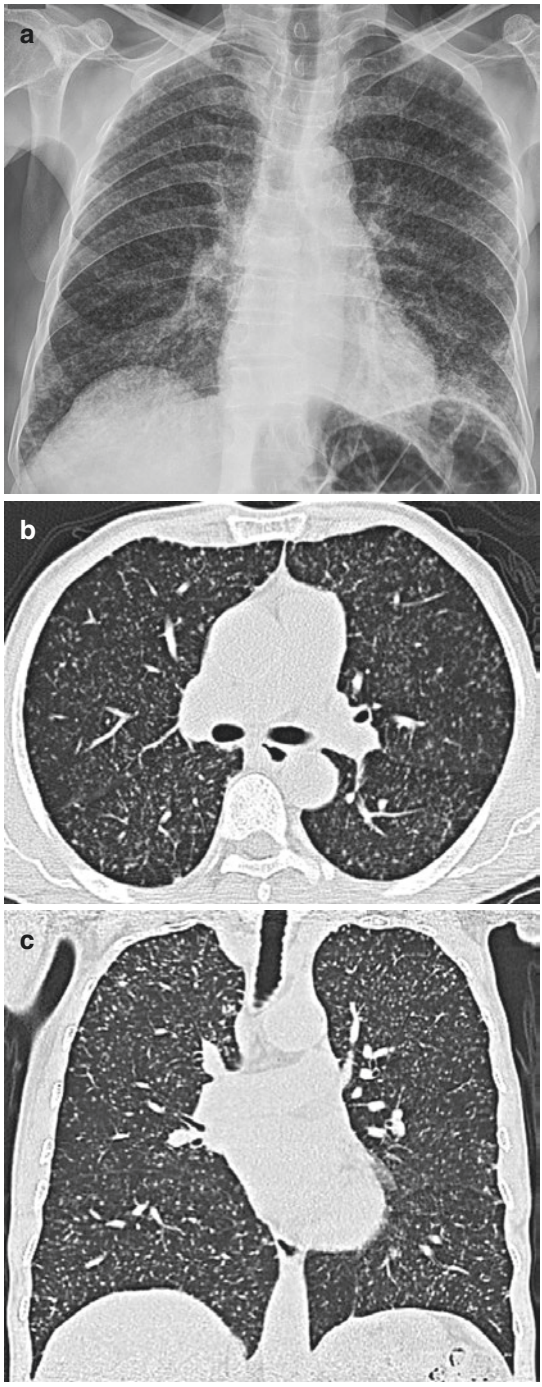

Fig. 5.5 (**a**–**c**) Chest X-ray and HRCT (axial and coronal) of a 41-year-old man with miliary tuberculosis show soft tissue opacity random micronodules

Tree-in-bud. Defined as the presence of centrilobular linear branching densities. It may suggest TB in cases with associated apical cavitation (in immunocompromised patients) (Fig. 5.6).

Halo sign. Related to the presence of a ground-glass halo around a nodule, mass, or consolidation. In the context of a neutropenic immunocompromised patient, it can be associated to invasive mycosis (aspergillosis, mucormycosis).

The identification of microorganisms in patients with CAP varies according to the series. In a recent US series (patients with CAP who required hospitalization), a pathogen was identified in 38% of the cases, with a higher frequency of viral infection (23%) over bacterial infection (11%) [7].

Microorganisms frequently causing pneumonia and sepsis of pulmonary origin are described, with their main radiographic manifestations (Fig. 5.7).

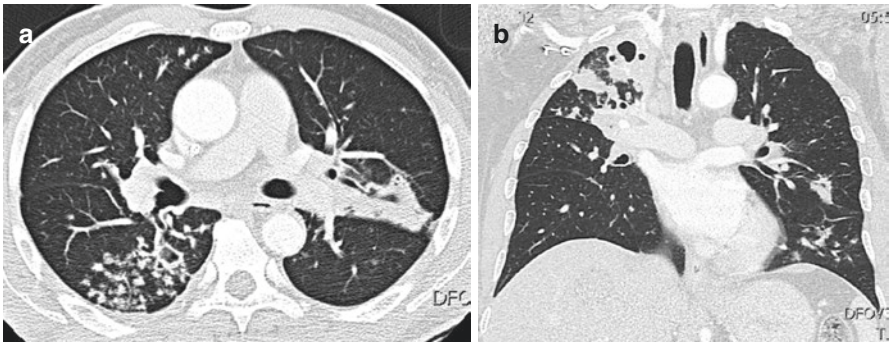

Fig. 5.6 (**a**, **b**) Axial and coronal HRCT of a 49-year-old man with tuberculosis shows centrilobular nodules, tree-in-bud opacities and upper right cavitation

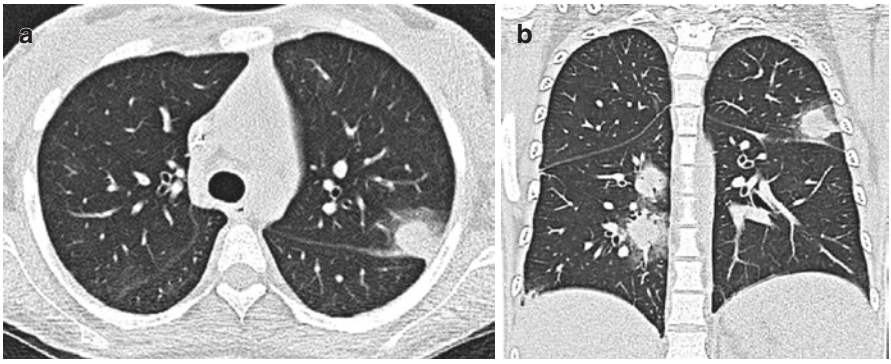

Fig. 5.7 (**a**, **b**) Halo sign. Axial and coronal HRCT of a 20-year-old woman with invasive pulmonary aspergillosis shows ground-glass opacity surrounding soft tissue nodules

Virus

Viruses represent the most frequent cause of respiratory infections in children and adults. In immunocompetent patients, most respiratory viral infections are self-limited. However, in a group of immunocompetent patients and in immunocompromised patients, respiratory viral infections present with severe tracheobronchitis, bronchiolitis, or pneumonia. The direct cytopathic effect of the virus causing damage to the respiratory epithelium can be associated to necrotizing bronchitis/bronchiolitis, diffuse alveolar damage, and/or alveolar hemorrhage. The manifestations of viral pneumonia on imaging studies depend on the degree of airway and/or lung parenchymal alteration and on the association of permeability pulmonary edema or alveolar hemorrhage. X-ray findings include normal X-ray, bronchial wall thickening, ill-defined nodules, and "patches" of peribronchovascular consolidation. HRCT may show ground glass, consolidation, thickening of peribronchovascular interstitium, thickening of interlobular septum, nodules tree-in-bud pattern, and areas of focal air entrapment with mosaic attenuation pattern [8].

Influenza virus type A is the most important respiratory virus in the general population. According to OMS, data between 10% and 20% of the world population is infected each year by the influenza virus. The mortality associated to the seasonal influenza type A virus occurs mainly in patients over 65 years. However, in the recent influenza A virus (H1N1) pandemic originated in Mexico, severe cases of pneumonia occurred in younger patients, pregnant women and obese patients. Radiographic manifestations of influenza pneumonia vary among the different series. In the study by Kloth et al. on 56 patients (36 immunocompromised and 20 immunocompetent) with influenza pneumonia, the most frequent HRCT findings included centrilobular nodules (69.6%), tree-in-bud (50%), and bronchial wall thickening (30.3%). In the group of immunocompromised patients, lung parenchymal alterations prevailed, and in the group of immunocompetent patients, the most frequent alterations were found in the airways. No differences in HRCT alterations were found between the different types and subtypes of influenza virus [9] (Fig. 5.8).

Respiratory infections due to adenovirus can present with severe pneumonia in immunocompetent patients. Sixty percent of the patients with adenovirus pneumonia require mechanical ventilation. Radiographic manifestations are similar to those of bacterial pneumonia with focal consolidation that progresses to bilateral consolidation, associated to ground-glass opacities and pleural effusion [10].

In immunocompromised patients, cases of pneumonia due to herpes simplex virus (HSV), varicella-zoster virus (VZV), and cytomegalovirus (CMV) have been described, as well as respiratory syncytial virus (RSV) or adenovirus (ADV).

In a series by Mayer et al. including 51 immunocompromised patients with clinical pneumonia and positive syncytial respiratory virus (RSV) tests, the most fre-

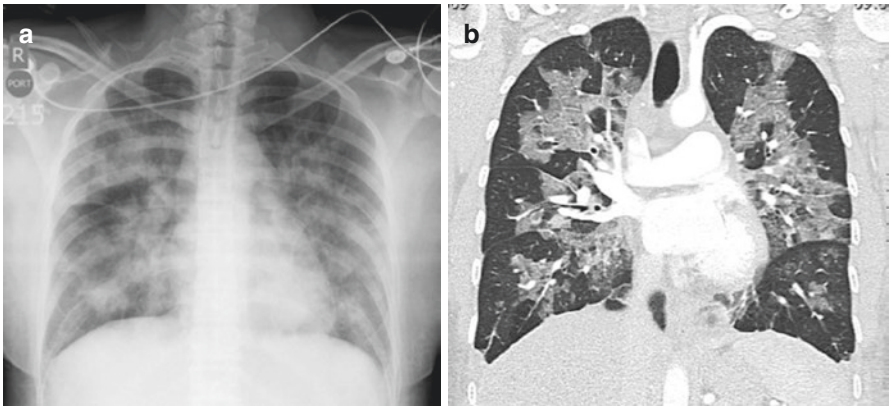

Fig. 5.8 (**a**, **b**) Chest X-ray and coronal HRCT of a 47-year-old woman with influenza (H1N1) infection show ground-glass opacities and multilobar consolidation

quent findings in the early stages of the disease were nodules and tree-in-bud pattern. With disease progression, ground glass (64%), consolidation (56%), and small nodules (55%) were described as relevant findings. The association of sinusitis, risk factors, and the radiographic manifestations described may suggest the diagnosis RSV pneumonia [11].

S. pneumoniae

It is the most frequent cause of bacterial CAP in most of the series. The characteristic radiographic pattern is of focal or lobar compromise, with consolidation predominantly affecting the inferior lobes. The clinical course is variable, with adequate response to antibiotics (in most patients) or with complications that include ARDS and death.

S. aureus

In recent years, respiratory infections due to methicillin-resistant (MRSA) and methicillin-sensitive (MSSA) *S. aureus* are considered as an important cause of severe CAP. In a multicenter study of 2259 adults hospitalized due to CAP, *S. aureus* was identified in 1.6% of the patients (0.7% MRSA and 1.0% MSSA). The incidence of MRSA was higher in patients undergoing chronic hemodialysis. The most frequent radiographic pattern in these patients is of bronchopneumonia, with bronchial wall thickening, ill-defined nodules, areas of peribronchovascular consolidation (multilobar and bilateral), and cavitation [12] (Fig. 5.9).

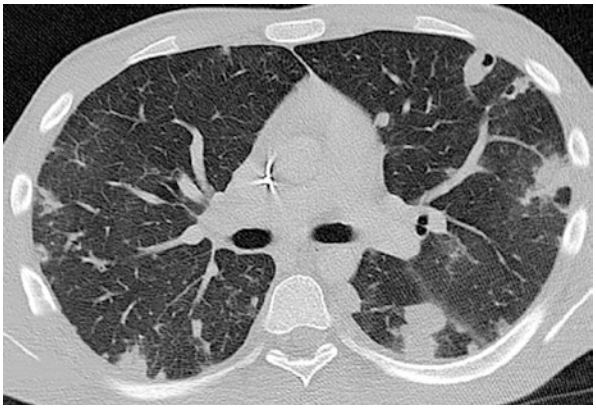

Fig. 5.9 Axial HRCT of a 32-year-old man with *S. aureus* infection shows subpleural nodules and cavitation

M. pneumoniae

M. pneumoniae is an important cause of pneumonia in adolescents and young adults. *M. pneumoniae* causes an interstitial inflammatory response by mononuclear cells appearing on the X-rays as perihilar and basal reticular opacities. The germ is an extracellular pathogen, whose survival depends on the adherence to the bronchial epithelium. For this reason, the bronchial wall thickening and the presence of centrilobular nodules are frequent findings in patients with *M. pneumoniae* pneumonia. Other HRCT findings include ground-glass opacities and consolidation [13]. The study by Miyashita et al. comparing rapid diagnostic tests for *M. pneumoniae* concluded that the ImmunoCard Mycoplasma kit was not useful to diagnose this entity and that in patients with three or four criteria of the Japanese respiratory society score, the findings on HRCT may suggest the diagnosis of *M. pneumoniae* [14].

M. tuberculosis

M. tuberculosis infection is an important cause of morbimortality associated to respiratory disease. It generally has a subacute or chronic course, but tuberculosis may manifest with acute respiratory clinical features, and differentiating it from respiratory infections of another etiology (bacterial) may prove difficult in the clinical practice.

The frequency of respiratory failure in patients with active TB ranges between 1.5 and 5%, with variable presentations (miliary TB-disseminated TB-ARDS). In a series by Mahmoud (350 patients with CAP admitted to the ICU), 3.1% of the patients developed ARDS associated to TB. In more than half of the patients, the suspicion of TB was based on radiographic manifestations [15].

The work by Yeh et al. to predict active pulmonary TB by means of the development of an HRCT score showed good performance with sensitivity (100%), specificity (96.9%), positive predictive value (76.5%), and negative predictive value (100%) [16].

Aspergillus

Invasive Aspergillus infection is an important cause of pulmonary sepsis in immunocompromised patients. It has been traditionally described in neutropenic patients. However, invasive aspergillosis has also been found in non-neutropenic patients (with COPD, in solid organ transplant recipients and in ICU patients). Radiographic manifestations of invasive aspergillosis are variable. In the angioinvasive form, radiographic manifestations include large nodules (with halo sign), consolidation, and cavitation. In aspergillosis with airway invasion (usually associated to parenchymal disease), the findings described include tree-in-bud, centrilobular nodules and consolidation [(17, 18).].

P. jiroveci

P. jiroveci pneumonia is described in immunocompromised patients due to HIV infection or in those immunocompromised without HIV infection (immunosuppression due to drug therapy, posttransplant, etc.). The clinical course is variable in the two groups (subacute in the first and acute in the second). In both groups, the main radiographic manifestation is the presence of ground-glass opacities with a geographic or diffuse pattern. Other less frequent manifestations include consolidation, crazy-paving pattern, cysts, intralobular lines, and nodules [19] (Fig. 5.10).

The most frequent complications associated to pneumonia, and that may be evaluated with imaging studies, correspond to secondary pleural infection, lung parenchymal necrosis (abscess), and ARDS.

Fig. 5.10 Axial HRCT of a 25-year-old man with *P. jiroveci* infection shows pulmonary cysts, right upper lobe consolidation, and right pneumothorax

Pleural Infection

The microbiology of pleural disease is different to that described in patients with CAP. In a multicenter study of intrapleural sepsis, the most common germs associated to pleural infection were *Streptococcus intermedius* (24%), *Streptococcus pneumoniae* (21%), and other *Streptococci* (7%), followed by anaerobic bacteria (20%) and staphylococci

(10%). The most common pathogens in hospital-acquired infections were staphylococci (35%) and gram-negative bacteria (23%) [20]. Ultrasound studies allow characterization of the pleural liquid and defining the presence of particles or septa and associated pleural thickening. CT allows defining the precise distribution of pleural collections, the presence of pleural thickening (with or without lung entrapment), and characterizing associated parenchymal alterations (Fig. 5.11).

Lung Abscess

It is defined as a circumscribed area of necrotic tissue or pus within the lung parenchyma that can cavitate and show an air-fluid level due to the occurrence of bronchopleural fistulas. Lung abscesses may be primary (generally related to aspiration) or secondary (due to bronchial obstruction) [21]. In imaging studies, lung abscesses appear as a mass with well-defined margins, cavitation (liquid or air densities within the lesion), and walls of variable thickness (according to time of evolution) (Fig. 5.12).

ARDS

Acute respiratory distress syndrome (ARDS) is a capillary permeability edema characterized by increased permeability of capillary endothelial cells and alveolar epithelial cells with refractory hypoxemia. The incidence of ARDS in patients with sepsis is 6% to 7% in Western Hemisphere countries. ARDS may be either primary or pulmonary (related to pneumonia /aspiration) or secondary or extrapulmonary (trauma, nonpulmonary sepsis, pancreatitis, etc.) [22]. Radiographic manifestations depend on the evolution of the ARDS and the degree of the lung's fibroproliferative response. During the early phases, imaging studies show ground-glass opacities and/or consolidation of variable distribution (patchy, AP attenuation gradient, or diffuse distribution). In patients with significant fibroproliferative changes, HRCT findings include ground-glass opacities, intralobular densities, distorted lung architecture, traction bronchiectasis, and honeycombing pattern. In a recent cohort of patients with ARDS, decreased respiratory compliance was associated to increased reticulation and traction bronchiectasis in an

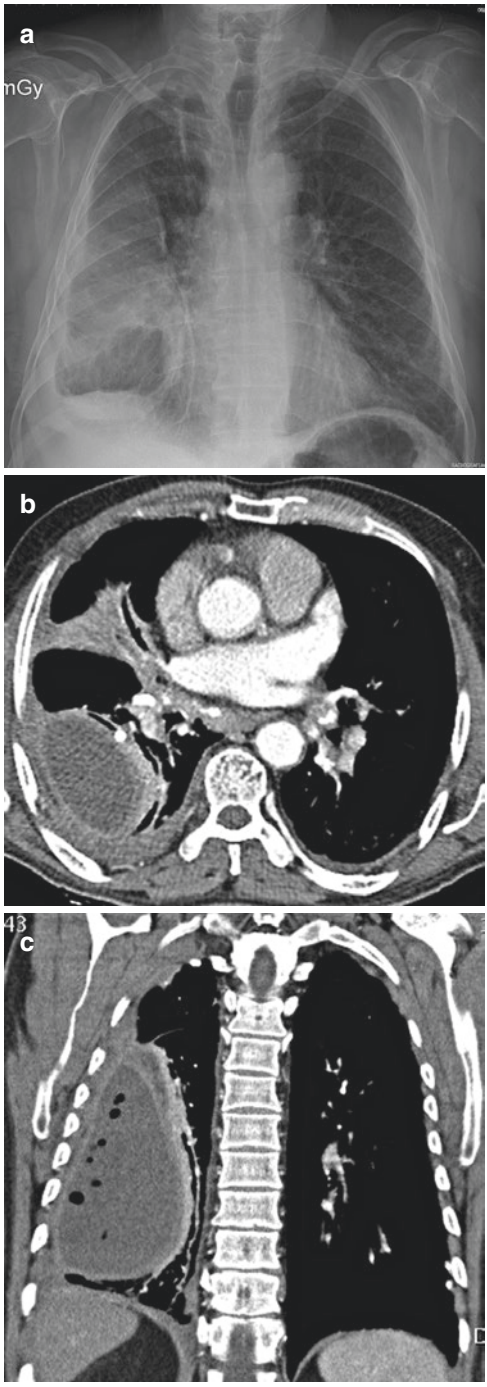

Fig. 5.11 (**a–c**) Chest X-ray and CT (axial and coronal) of a 56-year-old man with bacterial pneumonia and empyema show right pleural collection with air and pleural thickening

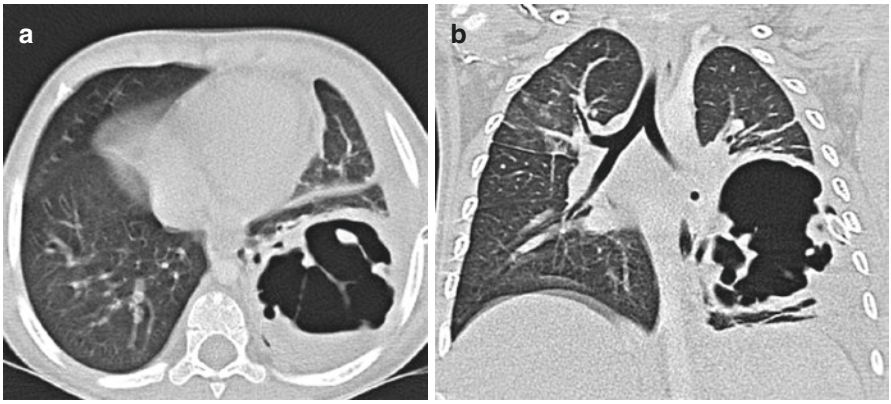

Fig. 5.12 (**a**, **b**) Axial and coronal HRCT of a 12-year-old boy with a pulmonary abscess shows cavitated mass in left lower lobe with air-fluid level

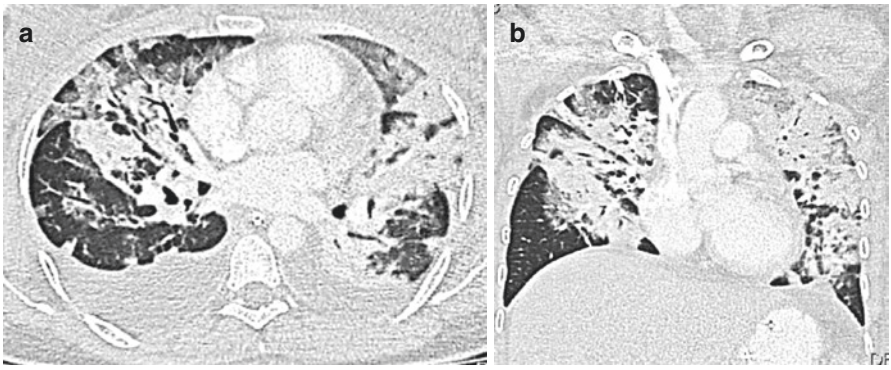

Fig. 5.13 (**a**, **b**) Axial and coronal HRCT of a 32-year-old woman with acute pyelonephritis and ARDS shows multilobar consolidation and bilateral pleural effusion

HRCT performed 14 days after the ARDS diagnosis. In theory, identification and quantification of fibroproliferative changes in HRCT can predict poor outcomes and a negative impact on ARDS patient's quality of life [23] (Fig. 5.13).

Differential Diagnosis

The list of imaging differential diagnoses for patients with pulmonary infection is long and includes disorders coursing with ground-glass opacities, consolidation, or nodules (most frequent findings in infectious disorders) such as small vessel pulmonary vasculitis, cryptogenic organizing pneumonia, chronic eosinophilic pneumonia, lipoid pneumonia, lymphoma, aspiration, and primary lung

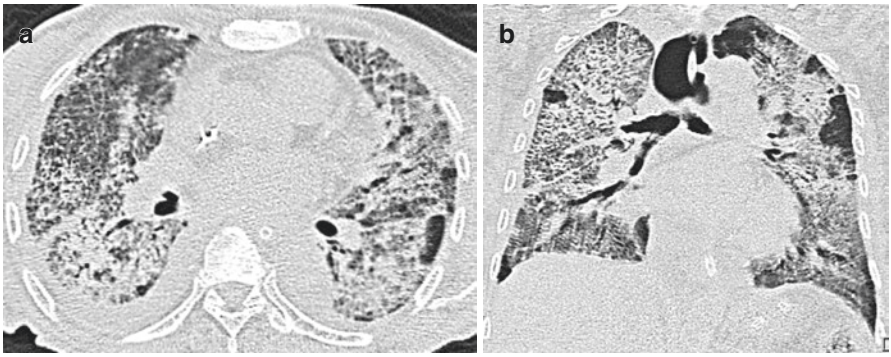

Fig. 5.14 (**a**, **b**) Axial and coronal HRCT of a 52-year-old woman with diffuse alveolar hemorrhage secondary to microscopic polyangiitis shows multilobar crazy-paving opacities and consolidation

adenocarcinoma. In cases of severe pulmonary infection with extensive parenchymal alterations or in those coursing with ARDS, among the differential diagnostic possibilities, pulmonary edema (of different etiologies), acute interstitial pneumonia, acute eosinophilic pneumonia, and diffuse alveolar hemorrhage must be considered (Fig. 5.14).

References

1. Singer M, Deutschman CS, Seymour CW, et al. The third international consensus definitions for sepsis and septic shock (sepsis-3). JAMA. 2016;315(8):801–10.
2. Wunderink RG, Waterer GW. Community-acquired pneumonia. N Engl Med. 2006;370(6): 543–51.
3. Morgan AJ, Glossop AJ. Severe community acquired pneumonia. BJA Educ. 2016;5:167–72.
4. Nie Y, Li C, Zhang J, et al. Clinical application of high resolution computed tomographic imaging features of community-acquired pneumonia. Med Sci Monit. 2016;22:1053–61.
5. Karhu JM, Ala-Kokko TI, Ahvenjärvi LK, et al. Early chest computed tomography in adult acute severe community acquired pneumonia patients treated in the intensive care unit. Acta Anaesthesiol Scand. 2016;60(8):1102–10.
6. Gharib AM, Stern EJ. Radiology of pneumonia. Med Clin North Am. 2001;85(6):1461–91.
7. Jain S, Self WH, Wunderink RG, et al. Community-acquired pneumonia requiring hospitalization among U.S. adults. N Engl J Med. 2015;373(5):415–27.
8. Franquet T. Imaging of pulmonary viral pneumonia. Radiology. 2011;260(1):18–39.
9. Kloth C, Forler S, Gatidis S, et al. Comparison of chest-CT findings of Influenza virus-associated pneumonia in immunocompetent vs.immunocompromised patients. Eur J Radiol. 2015;84(6):1177–83.
10. Tan D, Fu Y, Xu J, et al. Severe adenovirus community acquired pneumonia in immunocompetent adults: chest radiographic and CT findings. J Thorac Dis. 2016;8(5):848–54.
11. Mayer JL, Lehners N, Egerer G, et al. CT-morphological characterization of respiratory syncytial virus (RSV) pneumonia in immune-compromised adults. Rofo. 2014;186(7):686–9.
12. Self WH, Wunderink RG, Williams DJ, et al. Staphylococcus aureus community aquired pneumonia : prevalence, clinical characteristics, and outcomes. Clin Infect Dis. 2016;63(3):300–9.

13. Guo Q, Li HY, Zhou YP, et al. Associations of radiological features in mycoplasma pneumoniae pneumonia. Arch Med Sci. 2014;10(4):725–32.
14. Miyashita N, Kaway Y, Yamaguchi T, et al. Clinical potential of diagnostic methods for the rapid diagnosis of mycoplasma pneumoniae pneumonia in adults. Eur J Clin Microbiol Infect Dis. 2011;30(3):439–46.
15. Mahmoud ES, Baharoon SA, Alsafi E, et al. Acute respiratory distress syndrome complicating community acquired pneumonia secondary to mycobacterium tuberculosis in a tertiary care center in Saudi Arabia. Saudi Med J. 2016;37(9):973–8.
16. Yeh JJ, Chen SC, Chen CR, et al. A high-resolution computed tomography-based scoring system to differentiate the most infectious active pulmonary tuberculosis from community-acquired pneumonia in elderly and non-elderly patients. Eur Radiol. 2014;24(10):2372–84.
17. Kosmidis C, Denning DW. The clinical spectrum of pulmonary aspergillosis. Thorax. 2015;70(3):270–7.
18. Patterson KC, Strek ME. Diagnosis and treatment of pulmonary aspergillosis syndromes. Chest. 2014;146(5):1358–68.
19. Kanne JP, Yandow DR, Meyer CA. Pneumocystis jiroveci pneumonia: high-resolution CT findings in patients with and without HIV infection. Am J Roentgenol. 2012;198(6):555–61.
20. Maskell NA, Batt S, Hedley EL, et al. The bacteriology of pleural infection by genetic and standard methods and its mortality significance. Am J Respir Crit Care Med. 2006;174:817–23.
21. Kuhahda I, Zaragoulidis Tsirgogianni K, et al. Lung abscess-etiology, diagnostic and treatment options. Ann Transl Med. 2015;3(13):183.
22. Kim WY, Hong SB. Sepsis and acute respiratory distress syndrome: recent update. Tuberc Respir Dis (Seoul). 2016;79(2):53–7.
23. Burmham EL, Hyzy RC, Paine R III, et al. Detection of fibroproliferation by chest high-resolution CT scan in resolving ARDS. Chest. 2014;146(5):1196–204.